Supporting Information

Highly Active and Durable Hybrid Ni/NiOOH Catalyst by Synergistic High-Temperature Deposition and Electrochemical Oxidization for Hydrogen Evolution

Kebin Yang[1], Weibing Wu[1,*] and Yizhong Lu[1,*]

[1]School of Materials Science and Engineering, University of Jinan, Jinan, Shandong, China.

*Corresponding Authors

E-mail: mse_wuwb@ujn.edu.cn, mse_luyz@ujn.edu.cn

S1. Supplementary Figures

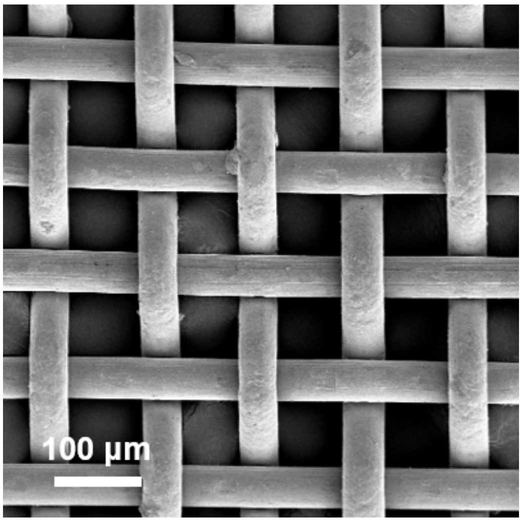

Fig. S1. SEM image for Cu mesh.

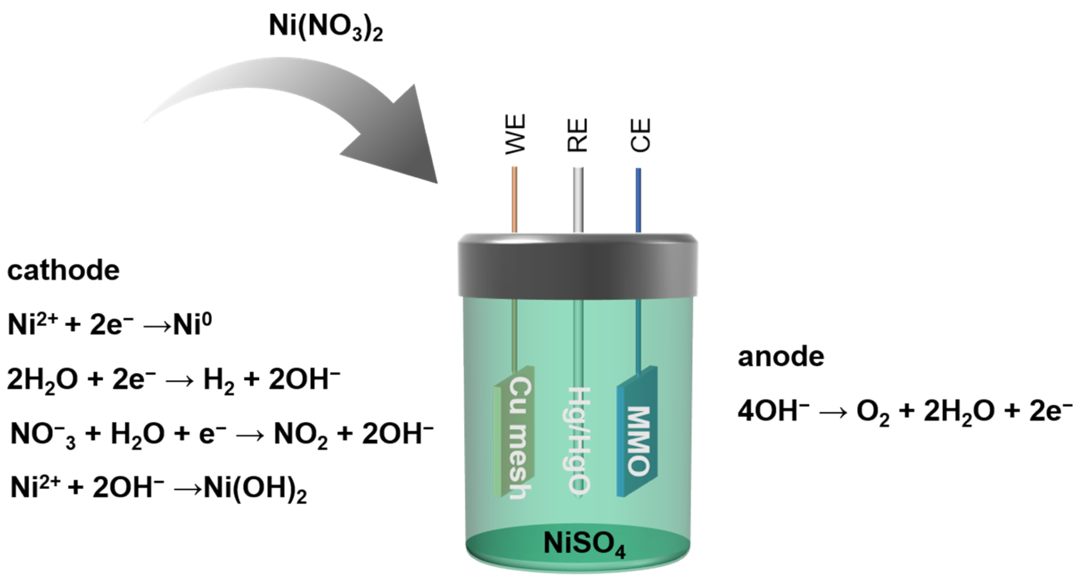

Fig. S2. The mechanism of $Ni/Ni(OH)_2$ precatalysts formation.

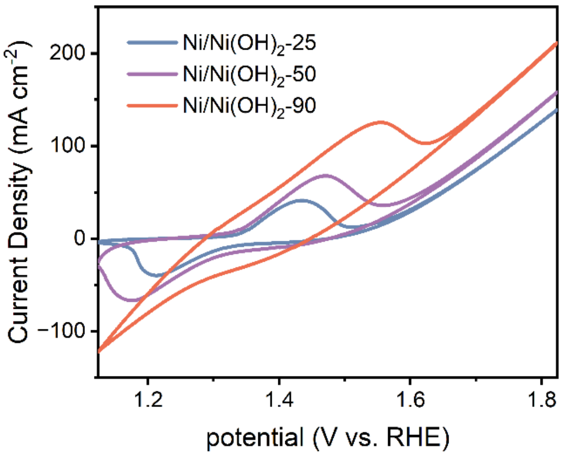

Fig. S3. oxidization CV curves for the $Ni/Ni(OH)_2$ precatalysts.

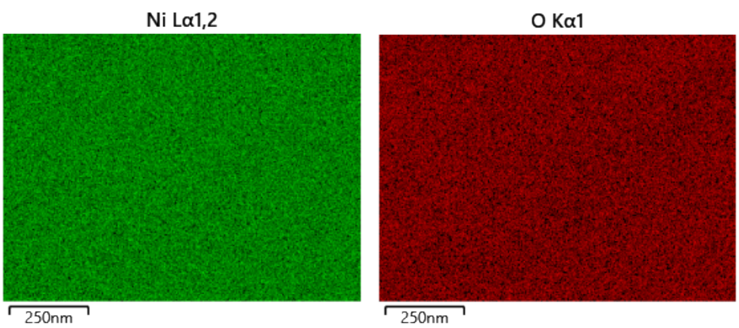

Fig. S4. The EDS-mapping of Ni/NiOOH-90.

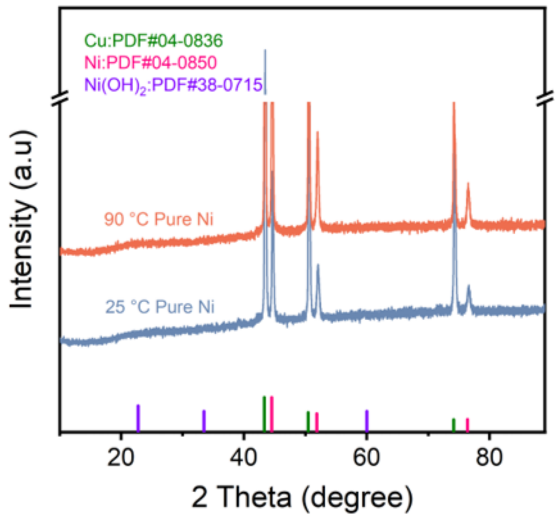

Fig. S5. XRD patterns of pure metal Ni.

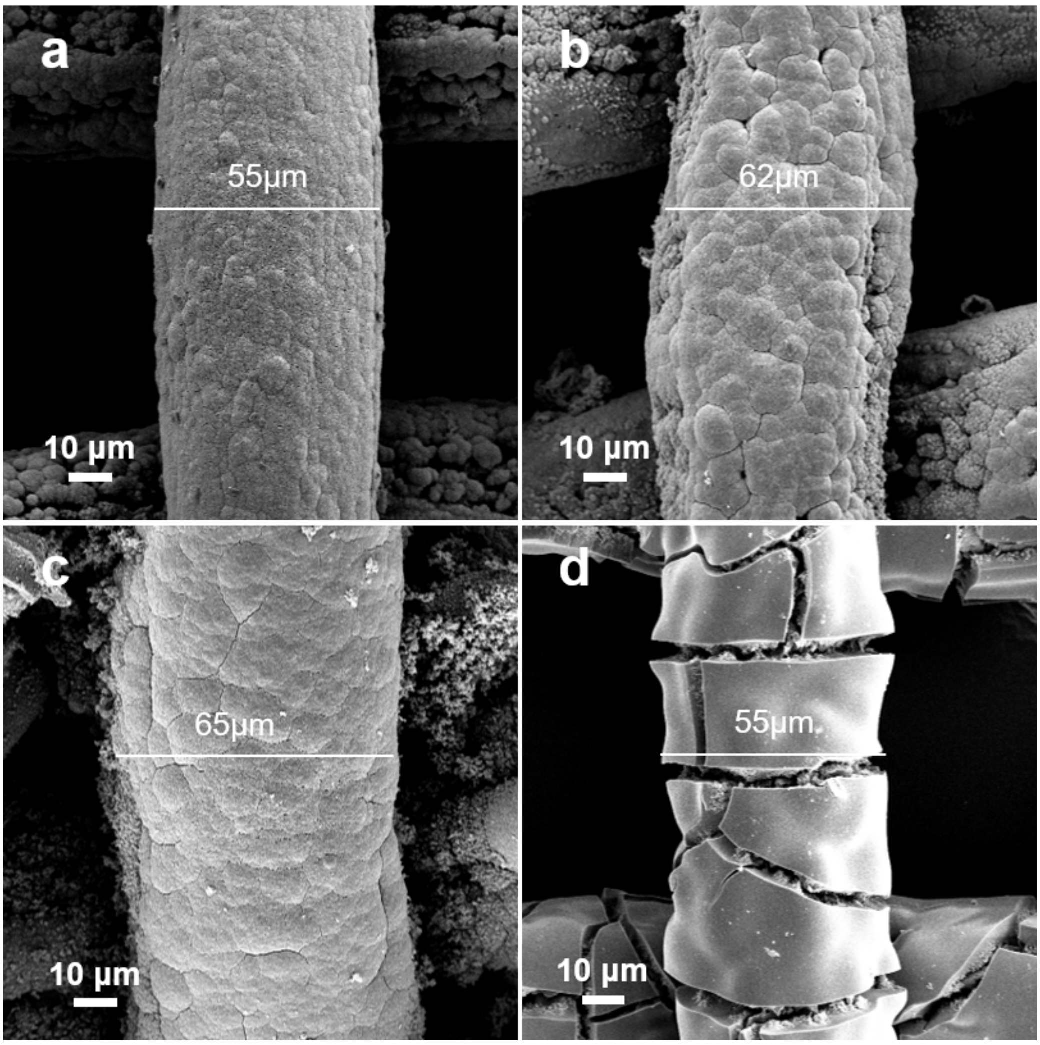

Fig. S6. SEM for varied loading amount. (a) Ni/NiOOH-90 deposited for 20 s. (b)

Ni/NiOOH-90 deposited for 50 s. (c) Ni/NiOOH-90 deposited for 100 s. (d) Ni/NiOOH-25 deposited for 300 s.

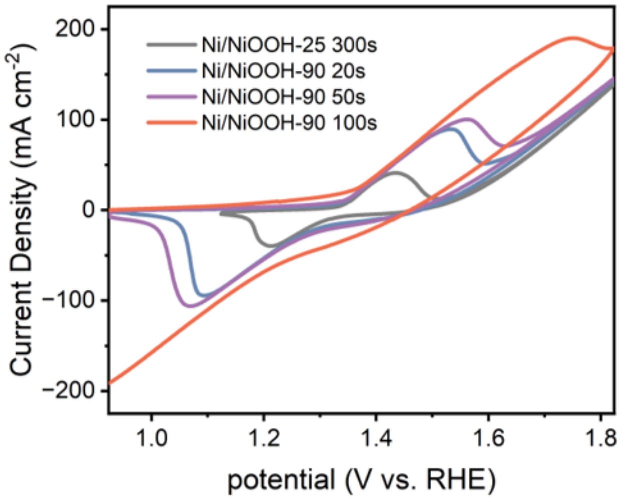

Fig. S7. Oxidization CV for varied loading amount.

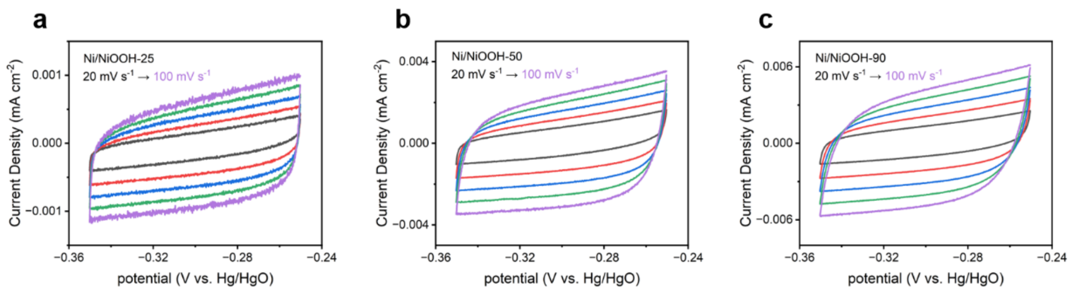

Fig. S8. Cyclic voltammogram as a function of scan rate.

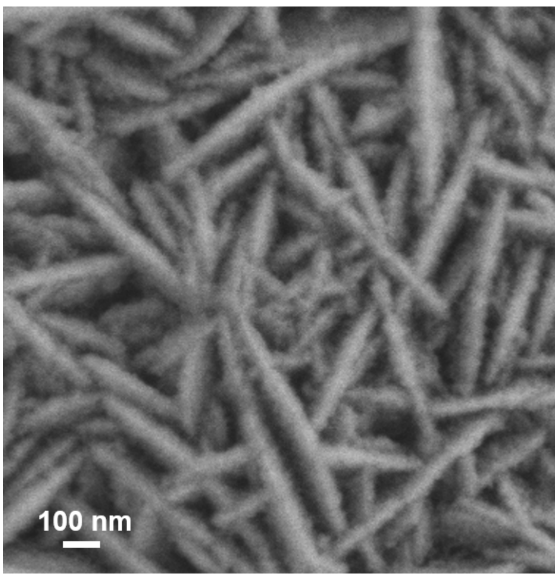

Fig. S9. SEM image for after stability test of Ni/NiOOH-90.

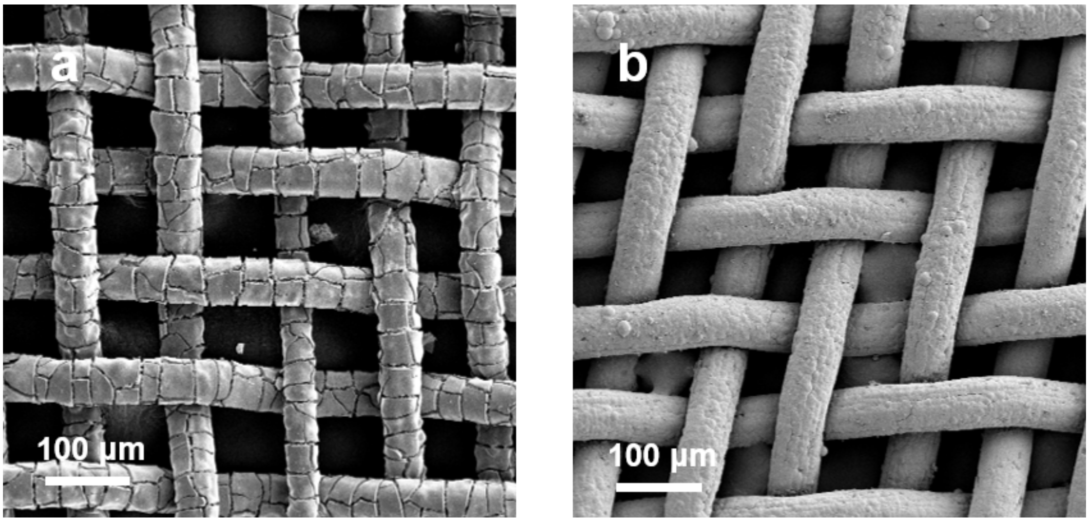

Fig. S10. SEM images for Ni/NiOOH-25 and Ni/NiOOH-90.

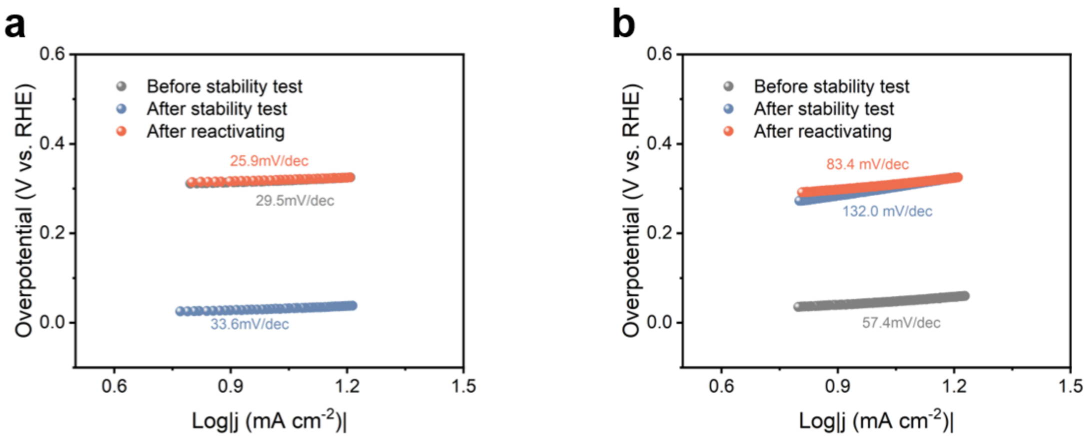

Fig. S11. The Tafel slope of (a) Ni/NiOOH-90 and (b) Ni/NiOOH-25.

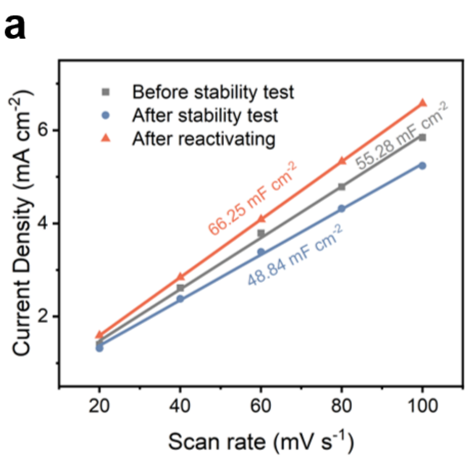

Fig. S12. Electrochemical double-layer capacitance of (a) Ni/NiOOH-90 and (b) Ni/NiOOH-25.

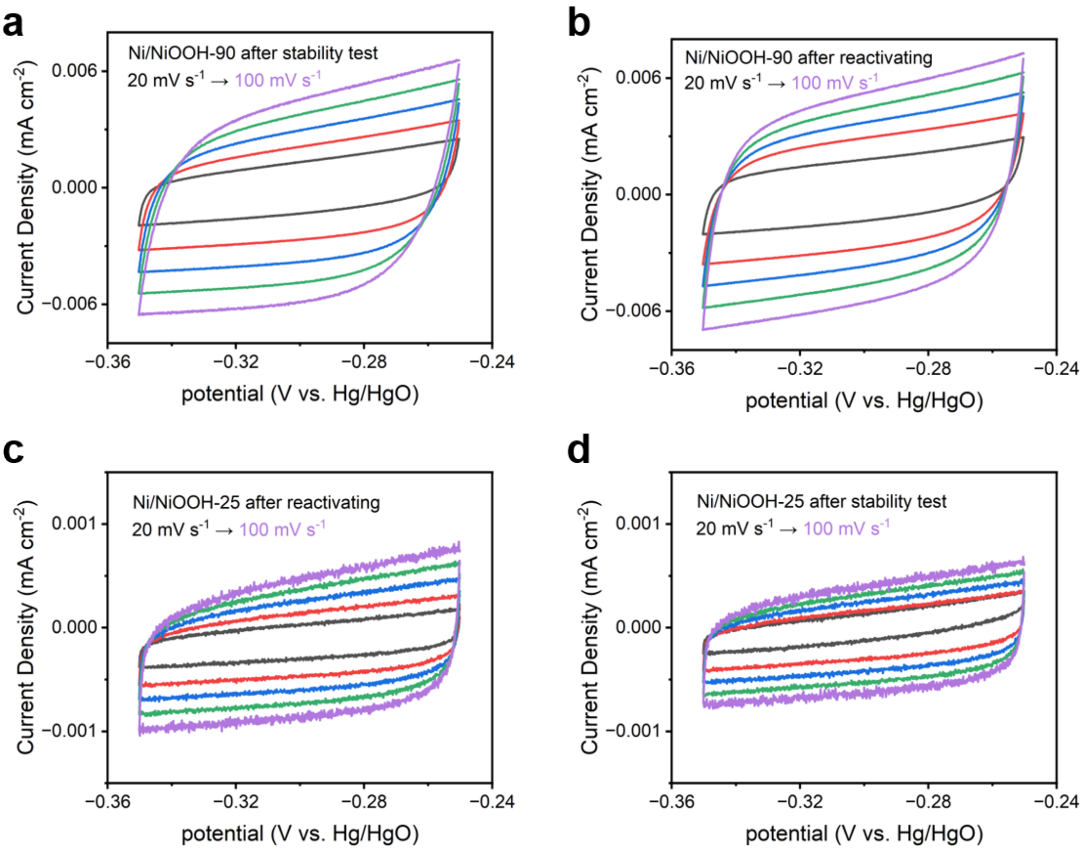

Fig. S13. Cyclic voltammogram as a function of scan rate.

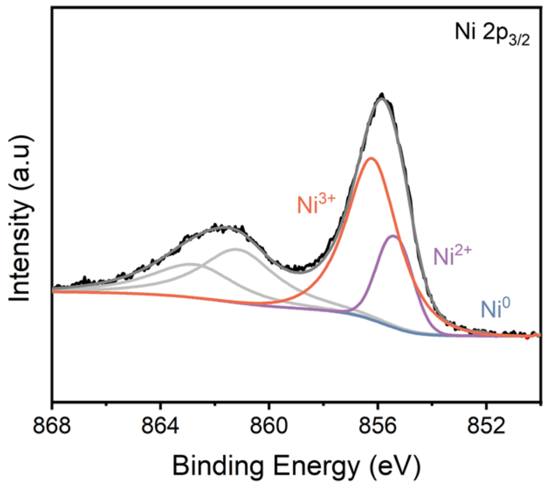

Fig. S14. XPS spectra of Ni/NiOOH-90 after reactivating.

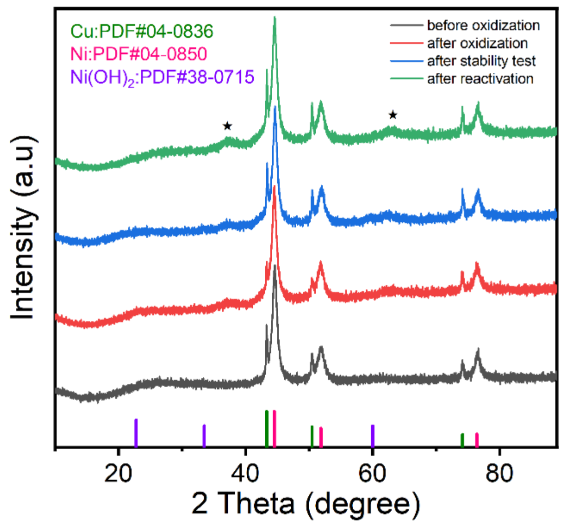

Fig. S15. XRD patterns of Ni/NiOOH-90.

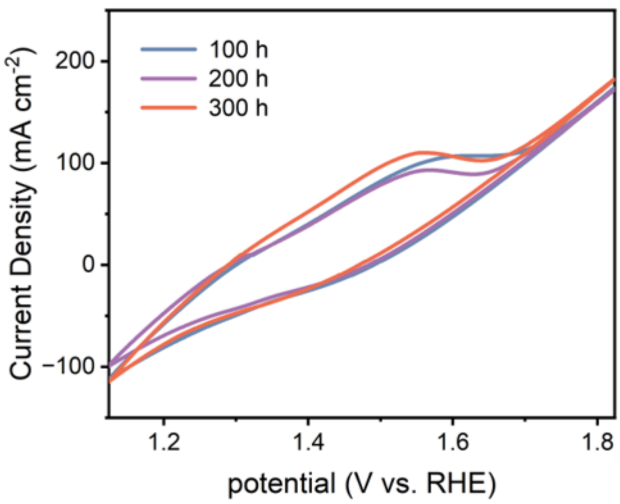

Fig. S16. oxidization CV curves for the Ni/NiOOH-90.

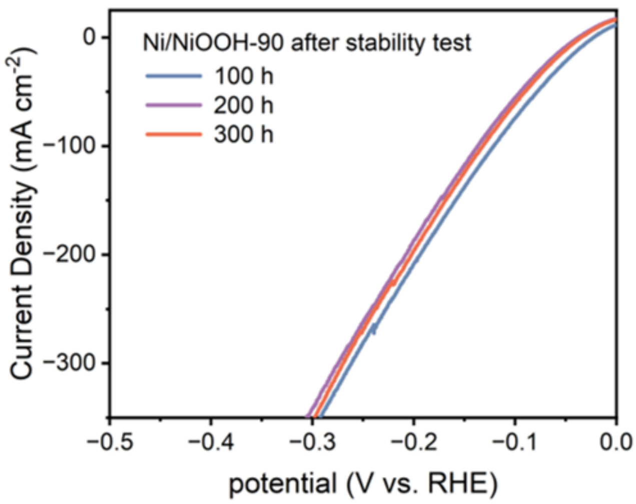

Fig. S17. LSV of samples with 90% iR-correction before reactivating.

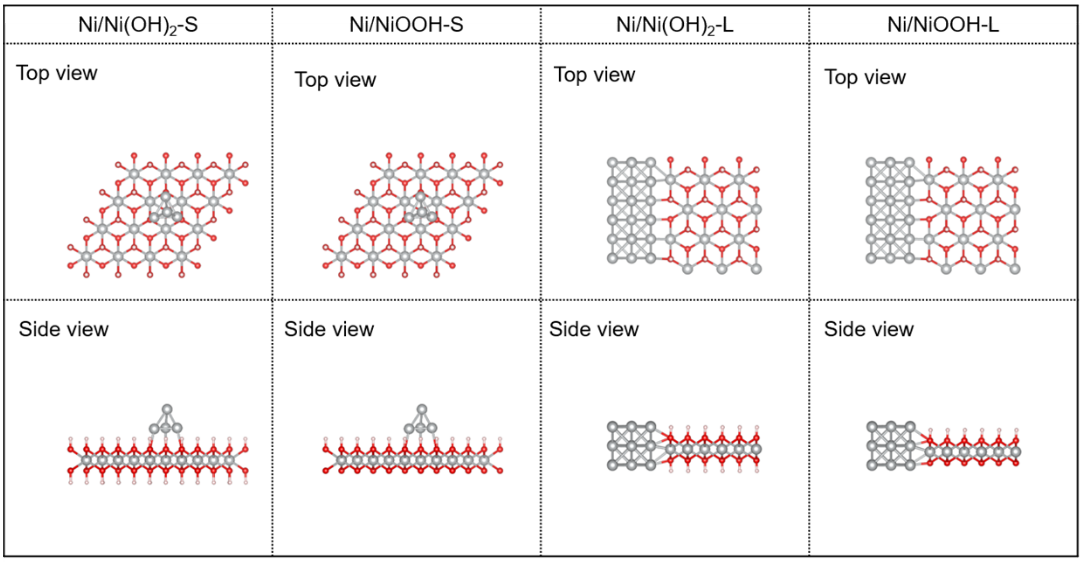

Fig. S18. The top and side view of the calculation models of Ni/$Ni(OH)_2$-S, Ni/NiOOH-S, Ni/$Ni(OH)_2$-L, and Ni/NiOOH-L.

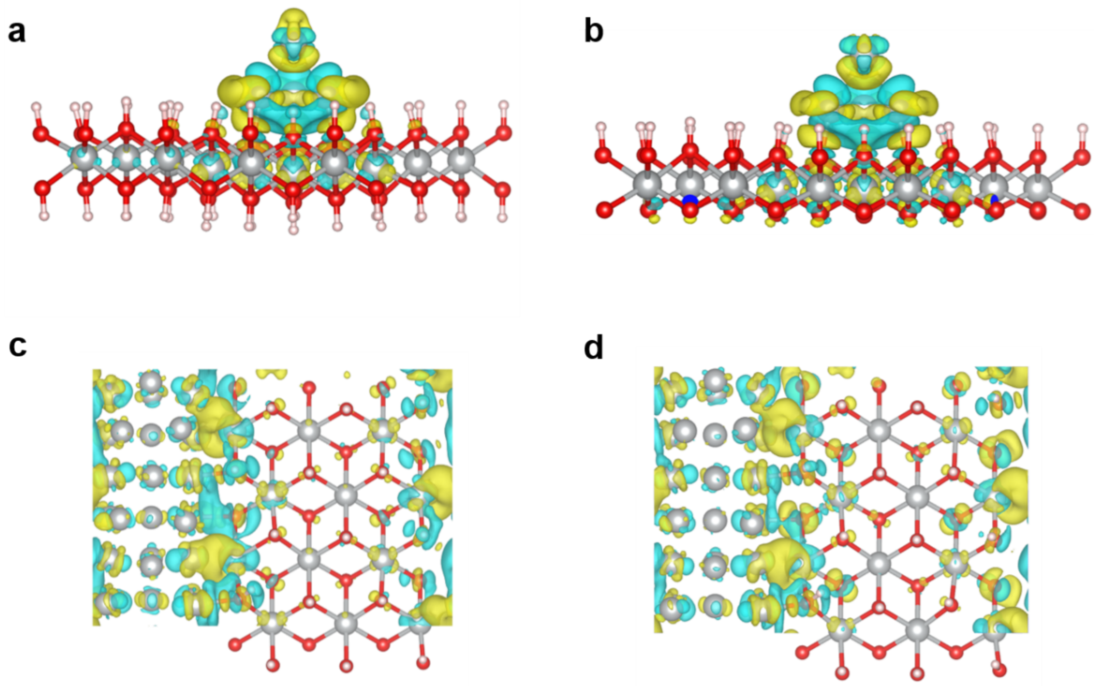

Fig. S19. The differential charge density of (a) $Ni/Ni(OH)_2$-S, (b) Ni/NiOOH-S, (c) $Ni/Ni(OH)_2$-L, and (d) Ni/NiOOH-L.

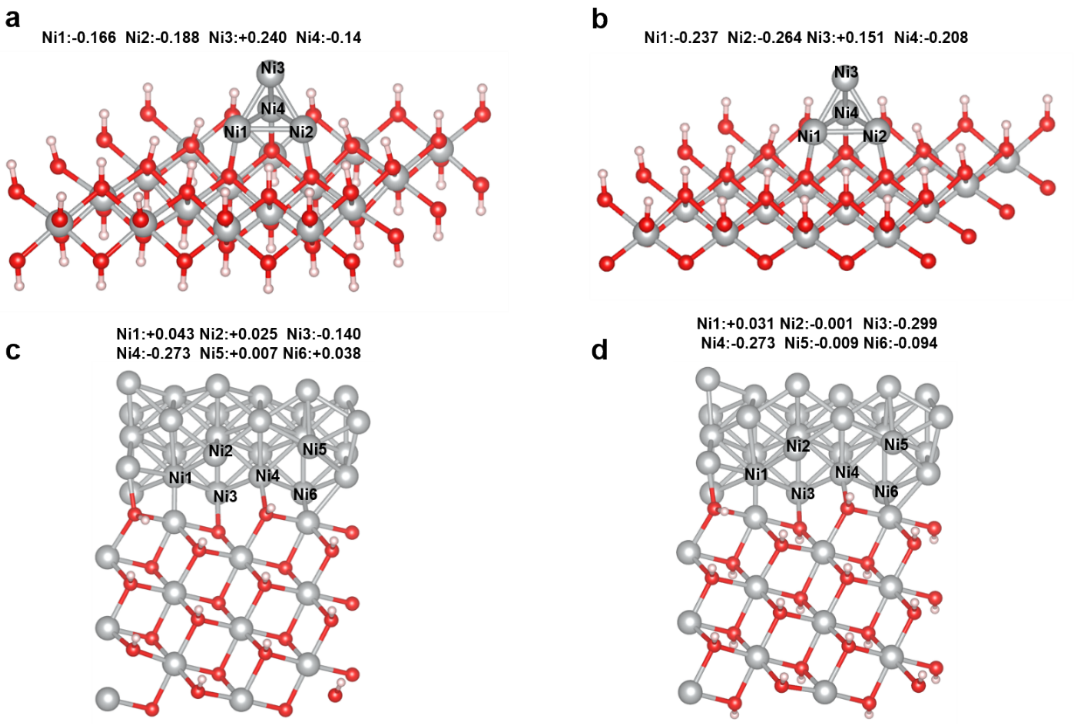

Fig. S20. The Bader charge analyses of (a) $Ni/Ni(OH)_2$-S, (b) Ni/NiOOH-S, (c) $Ni/Ni(OH)_2$-L, and (d) Ni/NiOOH-L.

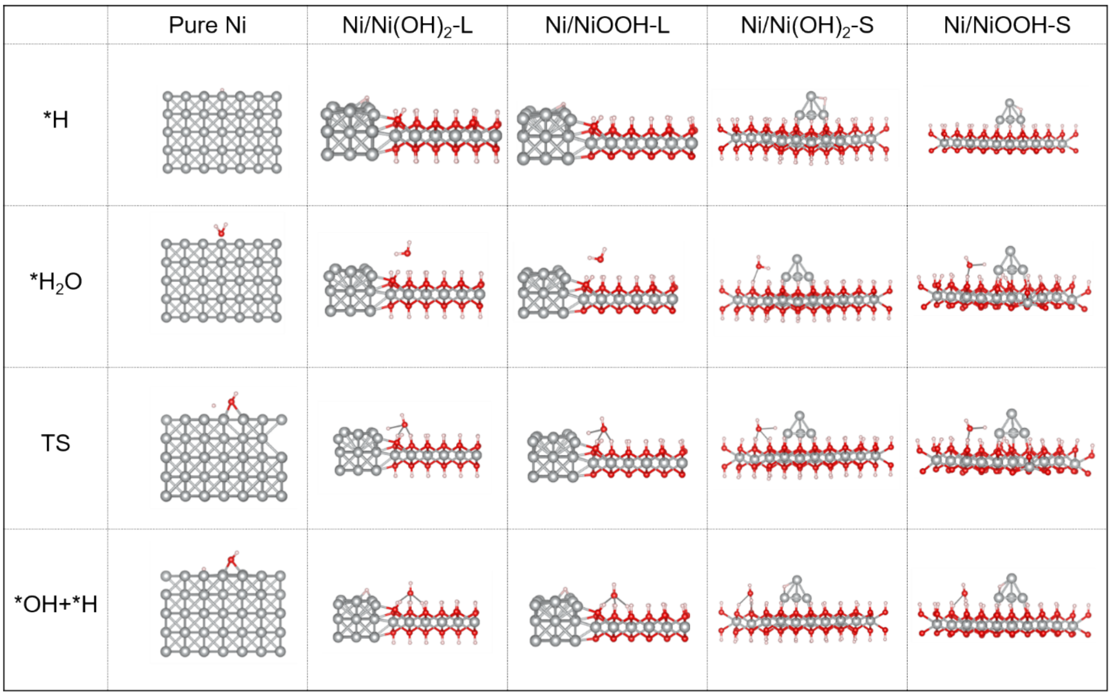

Fig. S21. The DFT calculation models of Pure Ni, Ni/Ni(OH)$_2$-L, Ni/NiOOH-L, Ni/Ni(OH)$_2$-S, and Ni/NiOOH-S.

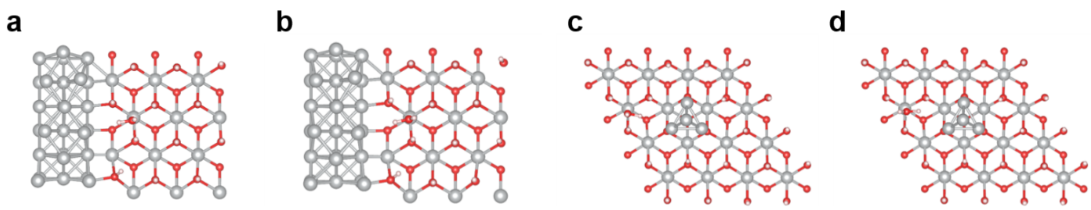

Fig. S22. The top and side view of the calculation models of H2O adsorption on (a) Ni/Ni(OH)$_2$-S, (b) Ni/NiOOH-S, (c) Ni/Ni(OH)$_2$-L, and (d) Ni/NiOOH-L.

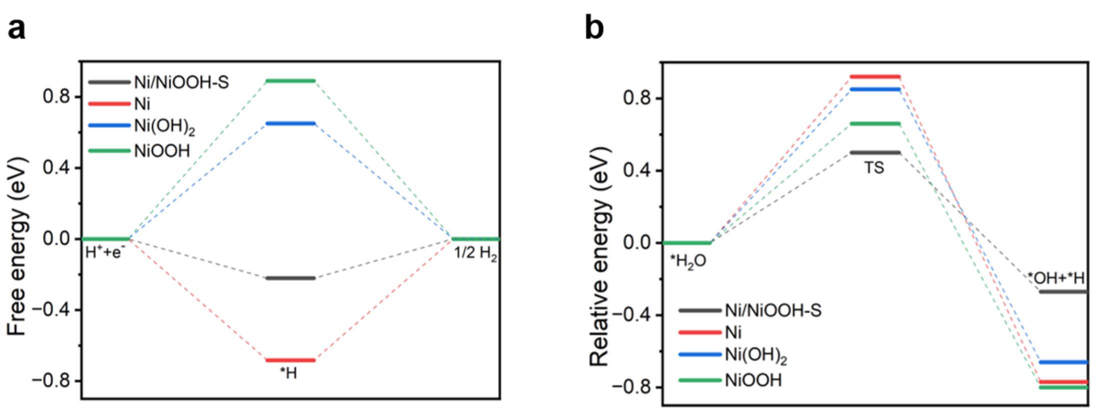

Fig. S23. (a) The calculated Gibbs free energy of *H at different sites on different models. (b) Potential energy profile of $*H_2O$ dissociation on different models.

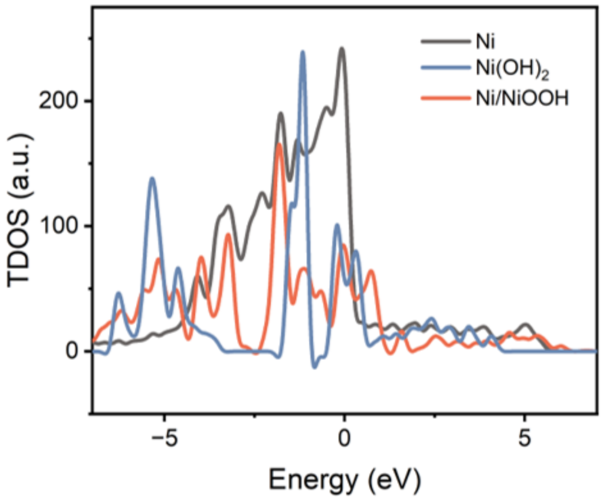

Fig. S24. The DOS of Ni, $Ni(OH)_2$, and Ni/NiOOH.

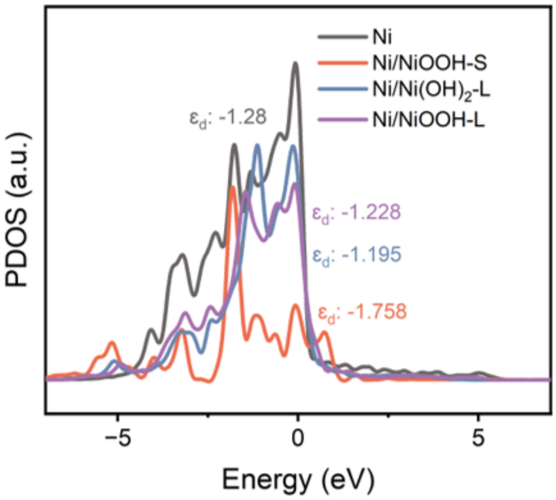

Fig. S25. The d-band DOS of Ni, Ni/NiOOH-S, Ni/NiOOH-L and Ni/NiOOH-L.

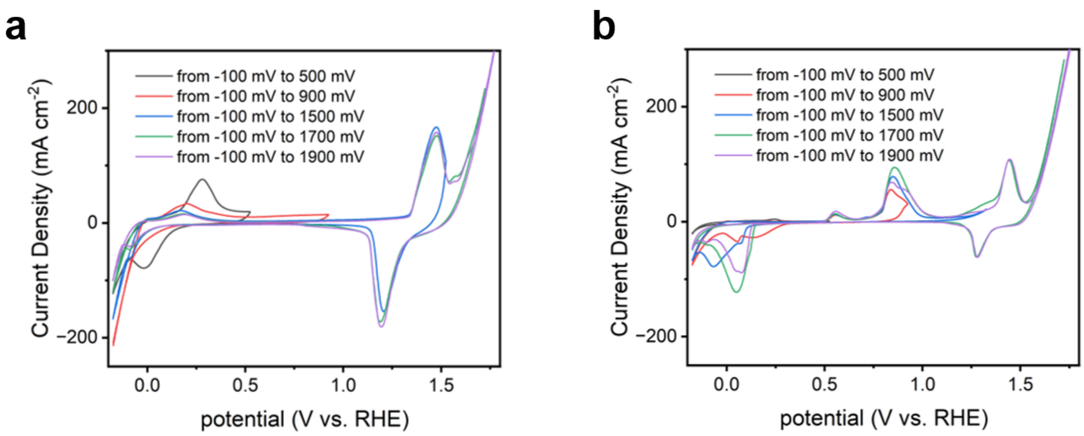

Fig. S26. CV curves of the precatalysts (a) Ni/Ni(OH)$_2$-90 (b) Ni/Ni(OH)$_2$-25.

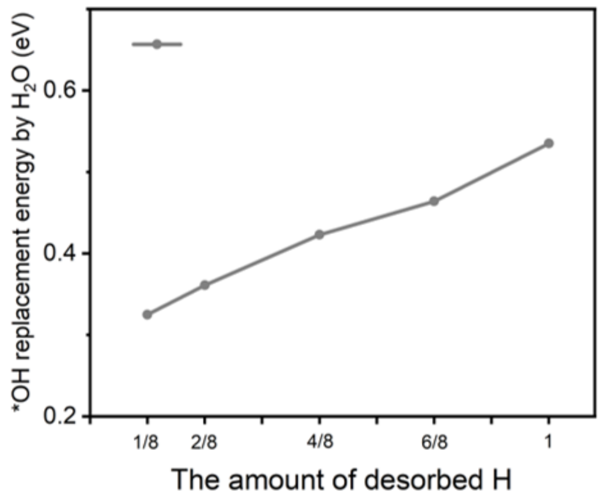

Fig. S27. The calculated *OH replacement energy by H_2O according to adsorption energies of *OH and H_2O.

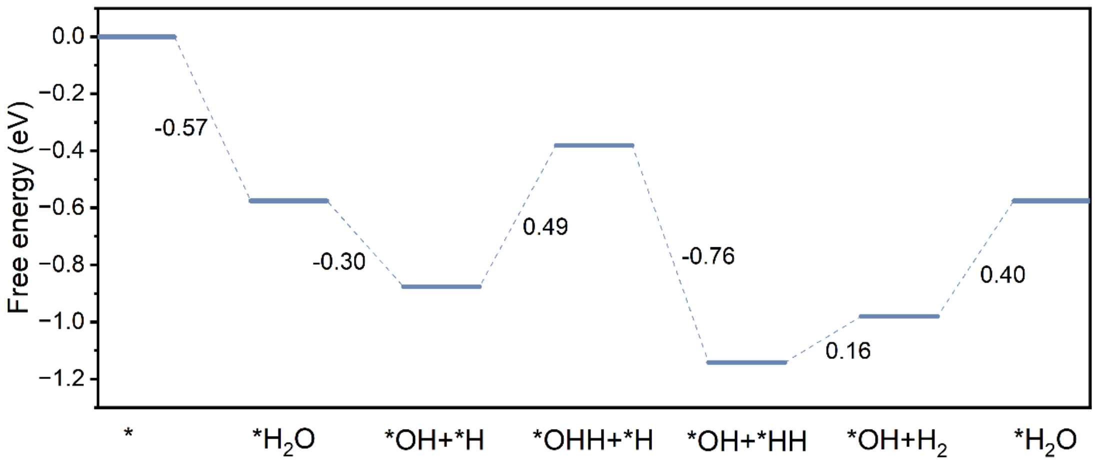

Fig. S28 Calculated free energy diagram for hydrogen migration path on Ni/NiOOH-S.

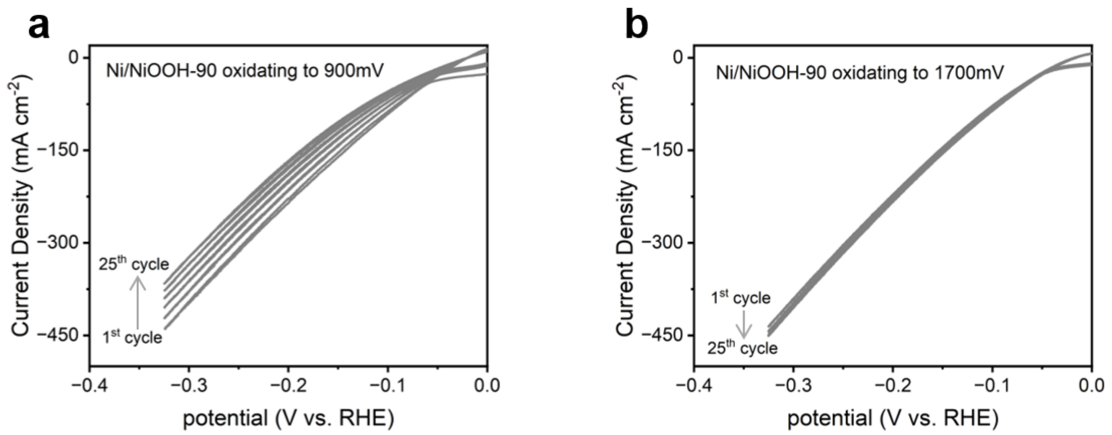

Fig. S29. Multiply CV curves of the samples. (a) Ni/NiOOH-90 oxidating to 900 mV. (b) Ni/NiOOH-90 oxidating to 1700 mV.

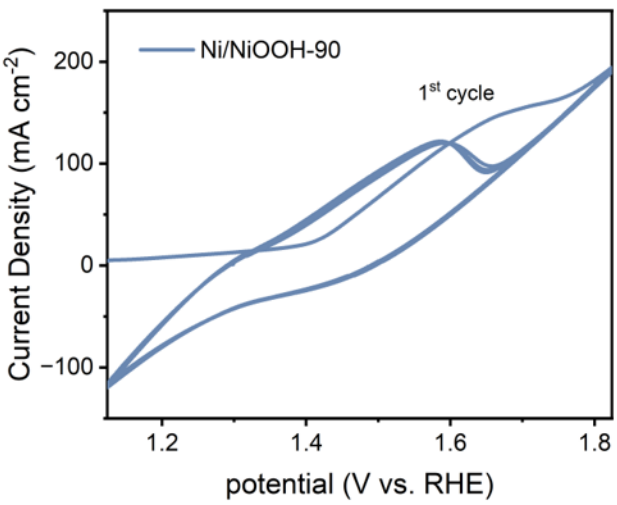

Fig. S30. Multiply oxidation CV of Ni/NiOOH-90.

S2. Supplementary Tables

Table S1. Comparison of HER performance in 1.0 M KOH for Ni/NiOOH with other catalysts.

Catalysts	Overpotential (mV, j=10 mA cm^{-2})	References
Ni/NiOOH	**30**	This work
NiCu/Ni(OH)$_2$	**23**	*Angew. Chem. 2022, 134, e202202518.* [1]
Ni/Ni(OH)$_2$	**30**	*international journal of hydrogen energy 46 (2021)*

(electrodeposition)		*26861 e26872.* [2]
N, Pt-MoS_2	38	*Energy Environ. Sci., 2022, 15, 1201-1210.* [3]
Ni/$Ni(OH)_2$ (hydrothermal)	39	*Adv. Mater. 2020, 1906915* [4]
Ni/$Ni(OH)_2$ (sintering)	40	*Adv. Energy Mater. 2025, 2406080* [5]
Ni/$Ni(OH)_2$ (electrodeposition)	57	*J. Mater. Chem. A, 2020, 8, 23323–23329* [6]
$Ni(OH)_2$@Ni-N/Ni-C/NF	60	*Nat Commun, 2023, 14:547.* [7]
Ni/$Ni(OH)_2$ (hydrothermal)	72	*Journal of Energy Chemistry 61 (2021) 236–242* [8]
Ni_2P/$NiMoO_x$	91	*ACS Catal. 2023, 13, 9792−9805* [9]
$Ni(OH)_2$@NM	135	*Applied Catalysis B: Environmental, 2023, 325: 122296.* [10]
$Ni(OH)_2$@NF	153	*Applied Catalysis B: Environmental, 2023, 325: 122296.* [10]

Catalysts	Stability test current (mA cm^{-2})	Stability test time (h)	References
Ni/NiOOH	2000	300	This work
NiCu/$Ni(OH)_2$	10	100	*Angew. Chem. 2022, 134, e202202518.* [1]
Ni/$Ni(OH)_2$ (electrodeposition)	10	24	*international journal of hydrogen energy 46 (2021) 26861 e26872.* [2]
Ni/$Ni(OH)_2$ (hydrothermal)	10	10	*Adv. Mater. 2020, 1906915* [4]
Pt/$Ni(OH)_2$	10	10	*Nat. Mater. 2023,22,1022-1029* [11]
Ni/$Ni(OH)_2$ (electrodeposition)	10	27	*J. Mater. Chem. A, 2020, 8, 23323–23329* [6]
Ni/$Ni(OH)_2$ (hydrothermal)	10	28	*Journal of Energy Chemistry 61 (2021) 236–242* [8]
Ni_2P/$NiMoO_x$	200	100	*ACS Catal. 2023, 13, 9792−9805* [9]
Ru/RuO_2	10	300	*Energy Environ. Sci., 2021, 14, 5433–5443* [12]
PtRu/RuO_2	250	100	*Nat. Commun. (2024) 15:1447*[13]
Ru@Cu−TiO_2/Cu	500	160	*J. Am. Chem. Soc. 2023, 145, 21419−21431* [14]
Ru/MoO_x	1000	200	*Adv. Energy Mater. 2023, 2301492* [15]

1. J. Wang, S. Xin, Y. Xiao, Z. Zhang, Z. Li, W. Zhang, C. Li, R. Bao, J. Peng, J. Yi and S. Chou, *Angew. Chem. Int. Ed.*, 2022, **61**, e202202518.
2. W. Lai, L. Ge, H. Li, Y. Deng, B. Xu, B. Ouyang and E. Kan, *Int. J. Hydrogen Energy*, 2021, **46**, 26861-26872.
3. Y. Sun, Y. Zang, W. Tian, X. Yu, J. Qi, L. Chen, X. Liu and H. Qiu, *Energy Environ. Sci.*, 2022, **15**, 1201-1210.
4. L. Dai, Z. N. Chen, L. Li, P. Yin, Z. Liu and H. Zhang, *Adv. Mater.*, 2020, **32**, 1906915.
5. W. Kuang, Z. Cui, C. Wang, T. Chen, Q. Wang, S. Li, T. Yang and J. Liu, *Adv. Energy Mater.*, 2025, **15**, 2406080.
6. J. Hu, S. Li, Y. Li, J. Wang, Y. Du, Z. Li, X. Han, J. Sun and P. Xu, *J. Mater. Chem. A*, 2020, **8**, 23323-23329.
7. K. Dastafkan, X. Shen, R. K. Hocking, Q. Meyer and C. Zhao, *Nat. Commun.*, 2023, **14**.
8. W. Zhong, W. Li, C. Yang, J. Wu, R. Zhao, M. Idrees, H. Xiang, Q. Zhang and X. Li, *J. Energy Chem.*, 2021, **61**, 236-242.
9. J.-T. Ren, L. Chen, H.-Y. Wang, W.-W. Tian, X.-L. Song, Q.-H. Kong and Z.-Y. Yuan, *ACS Catal.*, 2023, **13**, 9792-9805.
10. J. Zhang, J. Dang, X. Zhu, J. Ma, M. Ouyang and F. Yang, *App. Catal. B*, 2023, **325**, 122296.
11. C. Wan, Z. Zhang, J. Dong, M. Xu, H. Pu, D. Baumann, Z. Lin, S. Wang, J. Huang, A. H. Shah, X. Pan, T. Hu, A. N. Alexandrova, Y. Huang and X. Duan, *Nat. Mater.*, 2023, **22**, 1022-1029.
12. Y. Dang, T. Wu, H. Tan, J. Wang, C. Cui, P. Kerns, W. Zhao, L. Posada, L. Wen and S. L. Suib, *Energy Environ. Sci.*, 2021, **14**, 5433-5443.
13. Y. Zhu, M. Klingenhof, C. Gao, T. Koketsu, G. Weiser, Y. Pi, S. Liu, L. Sui, J. Hou, J. Li, H. Jiang, L. Xu, W.-H. Huang, C.-W. Pao, M. Yang, Z. Hu, P. Strasser and J. Ma, *Nat. Commun.*, 2024, **15**, 1447.
14. Y. Zuo, S. Bellani, G. Saleh, M. Ferri, D. V. Shinde, M. I. Zappia, J. Buha, R. Brescia, M. Prato, R. Pascazio, A. Annamalai, D. O. de Souza, L. De Trizio, I. Infante, F. Bonaccorso and L. Manna, *J. Am. Chem. Soc.*, 2023, **145**, 21419-21431.
15. Y. Zhang, C. Ma, X. Zhu, K. Qu, P. Shi, L. Song, J. Wang, Q. Lu and A. L. Wang, *Adv. Energy Mater.*, 2023, **13**, 2301492.